Journal of Building Engineering 113 (2025) 114094

Contents lists available at ScienceDirect

Journal of Building Engineering

journal homepage: www.elsevier.com/locate/jobe

A long short-term memory physics-informed neural network model for CO_2-based natural ventilation rate estimation

Sen Miao *, Marta Gangolells, Blanca Tejedor

Department of Project and Construction Engineering, Group of Construction Research and Innovation (GRIC), Universitat Politècnica de Catalunya, C/ Colom, 11, Ed. TR5, 08222, Terrassa, Barcelona, Spain

ARTICLE INFO

Keywords:
Natural ventilation rate
CO_2 tracer gas
Kalman filter
Long short-term memory
Physics-informed neural network

ABSTRACT

The occupant-released CO_2 tracer gas approach has been widely used for ventilation rate estimation. This approach is non-invasive, low-cost, and does not interfere with the occupants' activities. However, the CO_2 measurement noise and CO_2 generation uncertainties can significantly affect the accuracy of the estimated ventilation rates, while the dynamics of the natural ventilation rates could challenge the stability of the estimators. As commonly applied techniques, the moving average filter and the extended Kalman filter have their own advantages and limitations in addressing these issues. To further address the challenges in the natural ventilation rate estimation, this paper proposes a novel model named "NVR-PINN", based on the long short-term memory-physics-informed neural network and validates it with a case study. The proposed model combines the strengths of the moving average filter and the extended Kalman filter, demonstrating better practical values. It is capable of handling both CO_2 measurement noise and CO_2 generation uncertainty, effectively capturing the temporal dynamics of the natural ventilation rate, while processing the entire time series observation with a defined sequence window to yield more stable and consistent estimates. The analysis of the case study also revealed useful evidence for relevant research with regard to the applicability of existing ventilation rate estimation techniques.

List of abbreviations

MAF	Moving average filter
EKF	Extended Kalman filter
LSTM	Long short term memory
PINN	Physics informed neural network
NVR	Natural ventilation rate
IOT	Internet of Things

1. Introduction

Indoor air quality is one of the most important aspects of indoor environmental quality. Ventilation is the most common and

* Corresponding author.
E-mail address: sen.miao@upc.edu (S. Miao).

https://doi.org/10.1016/j.jobe.2025.114094
Received 19 May 2025; Received in revised form 8 September 2025; Accepted 12 September 2025
Available online 15 September 2025
2352-7102/© 2025 Elsevier Ltd. All rights are reserved, including those for text and data mining, AI training, and similar technologies.

effective way to maintain good indoor air quality. Relevant building standards, such as EN16798-1 [1] and ASHRAE 62.1 [2], specify the minimum ventilation rates required for different types of spaces, taking into account the characteristics and needs of the occupants. However, unlike mechanical ventilation systems, which operate at a controlled and stable ventilation rate, natural ventilation is driven by both buoyancy and wind effects, and is influenced by relevant building characteristics such as facade orientation and window geometry [3,4]. Therefore, the natural ventilation rate (NVR) often need to be estimated through field measurements.

The occupant-released CO_2 tracer gas approach is the most widely used method for ventilation rate estimation [5,6]. This approach uses CO_2 as a tracer gas to estimate the airflow rate based on the change in indoor CO_2 concentration over time using a mass balance equation (ASTM, 2018). Compared with direct measurements using airflow meters or other tracer gases such as SF6, the CO_2 tracer gas approach has many recognized advantages: it is non-invasive, low-cost, and most importantly, it does not disturb the indoor occupants due to the extensive setups for measurements [5,6]. Owing to these advantages, this method has been widely used to estimate ventilation rates in various naturally ventilated buildings, such as apartments [7,8], offices [9,10], and schools in particular [11–15].

Nevertheless, this approach has several limitations. Firstly and most importantly, the precision of the CO_2 measurement device has a substantial impact on the estimation results. Commercial CO_2 sensors typically have a measurement error of $\pm$50 ppm. The accuracy of the estimated ventilation rates can be significantly affected if the measurement noises are not properly addressed [5,16,17]. Commonly adopted solutions are to average the CO_2 observations over a period of time (e.g., 10 min) or to use a moving average filter (MAF) to filter out the noise in the CO_2 observations. [13–15,18–21]. These methods are simple and effective. However, they may compromise the time resolution and potentially misinterpret the results, as the measurement uncertainties are not properly addressed in a real sense. Moreover, the occupant-released CO_2 tracer gas method takes into account the amount of CO_2 generated by the occupants in the space. However, the CO_2 generation rate has uncertainties due to individual differences and activities of occupants. These methods do not account for the uncertainties associated with CO_2 generation.

The Bayesian filter (recursive Bayesian estimation) is an effective tool for addressing these limitations. As important members of the Bayesian filter family, the Kalman filter and extended Kalman filter (EKF) have been widely used to handle measurement noise since they were proposed in the 1960s, while they have also been used to estimate natural ventilation rates in various scenarios such as educational buildings and residential buildings [16,22–24]. However, the Kalman filter is based on the linear system, which is more suitable for steady-state estimation (i.e., stable, constant ventilation rates) rather than dynamic natural ventilation rates. The extended Kalman filter approximates a nonlinear system based on the Kalman filter, which has better stability for dynamic systems. However, since it is still based on “one-step-ahead” recursive prediction and updates, it is very sensitive to abrupt changes in CO_2 observations due to sudden window openings or changes in occupancy.

In fact, machine learning techniques have been widely used for modeling nonlinear dynamic systems. The long short-term memory (LSTM) model, a type of recurrent neural network designed specifically for sequence modeling, has demonstrated excellent capabilities in indoor CO_2 modeling [25–27]. However, the LSTM model is purely data-driven based on supervised learning, requiring a large amount of labeled data for training. Unlike state-space models such as the mass balance model, the LSTM model cannot learn to estimate the ventilation rates without observed ventilation rate data. In recent years, an emerging model named physics-informed neural network (PINN) has become a promising solution to this problem [28,29]. This technique incorporates governing physical laws (e.g., the mass balance equation) into the loss function. It learns to approximate the solution of differential equations, functioning as an advanced solver that integrate data-driven learning with physical laws. However, to the best of the author’s knowledge, no research has yet explored applying such techniques to estimate the natural ventilation rate.

Therefore, this paper proposes an LTSM-PINN model, named "NVR-PINN," for natural ventilation rate estimation. This model combines the advantages of the existing moving average filter (MAF) and the extended Kalman filter (EKF), providing more reliable natural ventilation rate estimation under the same conditions, while accounting for CO_2 measurement noise and uncertainty in the CO_2 generation rate. Certainly, these results contribute to both scientific knowledge and practical applications on this research topic.

Following this introduction, Section 2 elaborates on the methodology, Section 3 describes the case study, Section 4 analyzes and discusses the results, and Section 5 summarizes the conclusions and recommendations.

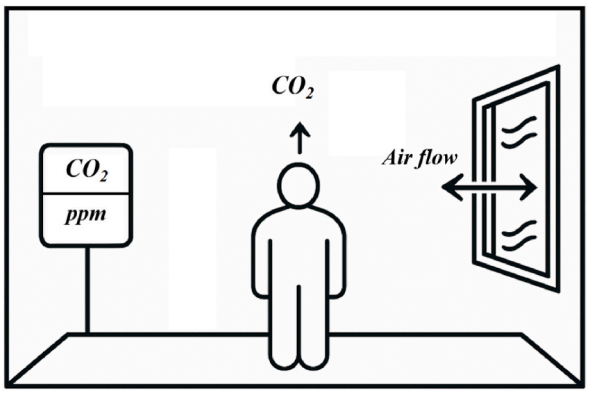

Fig. 1. Schematic diagram of the occupant-released CO_2 tracer gas approach.

2. Methodology

This section provides a step-by-step explanation, from the occupant-released CO_2 tracer gas approach (Section 2.1), to existing CO_2-based natural ventilation rate estimation techniques of the transient mass balance model (Section 2.2), moving average smoother (Section 2.3), and extended Kalman filter (Section 2.4). At the end, the proposed NVR-PINN is described in detail (Section 2.5).

2.1. Occupant-released CO_2 tracer gas approach

The tracer gas method is widely used to estimate ventilation rates. Unlike the traditional tracer gas methods, the occupant-released CO_2 tracer gas approach uses CO_2 generated by occupants. This avoids the external gas injection and extensive equipment setups that interfere with occupants' activities [5,6]. The airflow rate in a given space can be estimated based on the changes in indoor CO_2 concentrations over time (Fig. 1).

Notably, like other tracer gas methods, the occupant-released CO_2 tracer gas approach is also based on several fundamental assumptions (ASTM, 2018; [6]).

- The CO_2 is uniformly distributed in the space;
- The space is isolated, with an exclusive exchange with the outdoor air;
- The outside air is perfectly mixed within the space.

2.2. Transient mass balance model

In a given space of volume V, the concentration of CO_2 follows the law of mass balance. The ventilation rate can be calculated based on the difference in CO_2 concentrations between the indoor and outdoor air over a period of time, while taking CO_2 generation into account [5]:

$$\frac{dC_{in}}{dt} \cdot V = (C_{out} - C_{in}) \cdot Q_{vent} + N \cdot G \tag{1}$$

With a small time interval (e.g., dt = Δt = 1min), the transient mass balance equation can be expressed as:

$$C_{in,t} = C_{in,t-1} + \left(\frac{N_t \cdot G}{V} - \frac{Q_{vent,t}}{V} \left(C_{in,t-1} - C_{out,t} \right) \right) \cdot \Delta t \tag{2}$$

Where $C_{in,t}$ denotes indoor CO_2 concentration at time step t (ppm), $C_{in,t-1}$ is the indoor CO_2 concentration at previous time step t-1 (ppm), C_{out} is the outdoor CO_2 concentration (ppm), V is the room volume (m^3), N_t is the number of occupants in the room at time step t, G is the individual CO_2 generation rate (m^3/min/person), and Q_{vent} is the ventilation rate at time step t (m^3/min).

With known indoor and outdoor CO_2 concentrations, the number of occupants, and the individual CO_2 generation rate at each time step, corresponding ventilation rates can be calculated by a numeric solver.

2.3. Moving average filter

CO_2 observations often have noise due to the intrinsic measurement errors of CO_2 sensors. A simple and commonly used approach is to use a moving average filter (MAF) to filter out certain noises in CO_2 observations [18–21]. At each time step, the MAF computes the average of neighboring values of CO_2 observations within a defined window w. It then replaces the original CO_2 observation at the time step with this averaged value:

$$CO_2^*(t) = \frac{1}{w} \sum_{k=-\frac{w}{2}}^{\frac{w}{2}} CO_2(t+k) \tag{3}$$

Where t denotes the time step and w is the defined window length (e.g., 10 min).

The ventilation rate is then estimated based on the smoothed CO_2 observations using the transient mass balance equation:

$$C_{in,t}^* = C_{in,t-1}^* + \left(\frac{N_t \cdot G}{V} - \frac{Q_{vent,t}}{V} \left(C_{in,t-1}^* - C_{out,t}^* \right) \right) \cdot \Delta t \tag{4}$$

Notably, since MAF takes $w/2$ neighboring observations before and after any time step t to compute the average value, the smoothed CO_2 observations do not contain the initial and last $w/2$ observations, meaning that the smoothed data has a loss of observations for a w time length.

2.4. Extended Kalman filter

The extended Kalman filter (EKF) is a nonlinear extension of the well-known Kalman filter [30–32]. This technique is capable of

addressing CO_2 measurement noise while accounting for uncertainties associated with CO_2 generation rate. EKF works on a defined state-space model with "one-step-ahead" recursive estimation and updates. It estimates (predicts) the state of the system at the next time step, and then updates (or corrects) the state estimate with the new observation.

In a given space of volume V, the indoor CO_2 concentration follows the mass balance equation with a small time interval (Δt = 1min), so the system follows the dynamics:

$$C_{in,t+1} = C_{in,t} + \frac{N_t \cdot G_t}{V} - \frac{Q_{vent,t}}{V}\left(C_{in,t} - C_{out,t}\right) \tag{5}$$

$$Q_{vent,t+1} = Q_{vent,t} + w_{Qvent} \tag{6}$$

$$G_{t+1} = G_t + w_G \tag{7}$$

Where w_{Qvent} and w_G are the process noises that characterize the dynamics of the ventilation and CO_2 generation over time. Notably, the CO_2 generation rate has individual differences, so it comes from a uniform distribution rather than a fixed value:

$$G \sim U(G \cdot (1-u), G \cdot (1+u)) \tag{8}$$

Where u characterizes the individual differences in the CO_2 generation rate.

Hence, the state vector of the system at time step t can be expressed as:

$$X_t = \begin{bmatrix} C_{in,t} \\ Q_{vent,t} \\ G_t \end{bmatrix} \tag{9}$$

Where $C_{in,t}$ is the indoor CO_2 observation, while $Q_{vent,t}$ and G_t are hidden states (latent variables) of the system to be estimated.

The state of the system at the next time step *t+1* can be expressed as:

$$X_{t+1} = f(X_t) + w_t, w_t \sim N(0, Q) \tag{10}$$

Where $f(X_t)$ is the state transition function:

$$f(X_t) = \begin{bmatrix} C_{in,t} + \dfrac{N_t G_t}{V} - \dfrac{Q_{vent,t}}{V}\left(C_{in,t} - C_{out,t}\right) \\ Q_{vent,t} \\ G_t \end{bmatrix} \tag{11}$$

Q is the process noise covariance matrix:

$$Q = \begin{bmatrix} 0 & 0 & 0 \\ 0 & \sigma^2_{Qvent,p} & 0 \\ 0 & 0 & \sigma^2_{G,p} \end{bmatrix} \tag{12}$$

Since the system is nonlinear, EKF uses a first-order Taylor expansion to approximate state transition function around the previous state estimate $\widehat{X}_t$. Hence:

$$X_{t+1} \approx f(\widehat{X}_t) + F_t(X_t - \widehat{X}_t) + w_t \tag{13}$$

Where F_t is the Jacobian matrix:

$$F_t = \begin{bmatrix} 1 - \dfrac{Q_{vent,t}}{V} & -\dfrac{\left(C_{in,t} - C_{out,t}\right)}{V} & \dfrac{N_t}{V} \\ 0 & 1 & 0 \\ 0 & 0 & 1 \end{bmatrix} \tag{14}$$

The predicted state of the system is:

$$\widehat{X}_{t+1|t} = f(\widehat{X}_t) \tag{15}$$

The predicted covariance matrix is:

$$P_{t+1|t} = F_t P_t F_t^T + Q_t \tag{16}$$

Where P_t is the state covariance matrix characterizing the uncertainties between the states of CO_2, Q_{vent} and G, while Q_t is the process noise covariance.

EKF updates (corrects) the predicted state based on actual observations. The observation model of the system can be expressed as:

$$Z_t = HX_t + v_t, \quad v_t \sim N(0, R) \tag{17}$$

Where Z_t is the observation of the system, H is the observation matrix, and v_t is the measurement noise.

Since CO_2 is the only observed state of the system, the observation matrix $H = [1, 0, 0]$, $R = \sigma^2_{sensor}$, which is the variance of CO_2 sensor measurement error σ_{sensor}. Hence the system observation is:

$$Z_t = C_{observation,t} = C_{in,t} + v_t \tag{18}$$

The difference between the observed and predicted CO_2 concentration is called innovation in EKF, which can be expressed as:

$$Y_t = C_{observation,t} - C_{predicted,t} \tag{19}$$

$$C_{predicted,t} = C_{in,t|t-1} \tag{20}$$

The innovation covariance is:

$$S_t = HP_{t|t-1}H^T + R \tag{21}$$

Like a standard Kalman filter, EKF uses Kalman Gain to calibrate the estimate through observations, which can be expressed as:

$$K_t = P_{t|t-1}H^T S_t^{-1} \tag{22}$$

Hence, the state estimate can be updated:

$$X_{t|t} = X_{t|t-1} + K_t Y_t \tag{21}$$

The covariance matrix is also updated:

$$P_{t|t} = (I - K_t H)P_{t|t-1}(I - K_t H)^T + K_t R K_t^T \tag{22}$$

Where I is the identity matrix.

The above briefly describes the principle of EKF. For more detailed instructions on this technique, Labbe [32] is a very useful reference. Duarte et al. [16] first constructed and implemented an EKF for natural ventilation rate estimation with MATLAB. The EKF built in this research is generally the same, but additionally takes into account the individual differences of the CO_2 generation rate to better characterize and represent reality.

Notably, the initial values for the system states need to be assumed to initialize the EKF. In practice, the assumed initial values only affect the first few estimates. After several rounds of iterations, the EKF can automatically calibrate and track the state of the system.

2.5. NVR-PINN

The proposed NVR-PINN is a neural network architecture that integrates long short-term memory (LSTM) and physics-informed neural network (PINN) for natural ventilation rate estimation. LSTM is a type of recurrent neural network architecture designed specifically for sequential (time series) data [33]. LSTM can retain information across multiple time steps, enabling the model to capture temporal dependencies and context over time rather than relying solely on the current input. However, it is primarily a supervised learning model, which requires a large amount of labeled data for model training. PINN is an emerging neural network architecture that incorporates physical laws expressed by ordinary differential equations or partial differential equations into model training, which can be understood as a universal function approximator [28]. By embedding physical laws as a form of regularization,

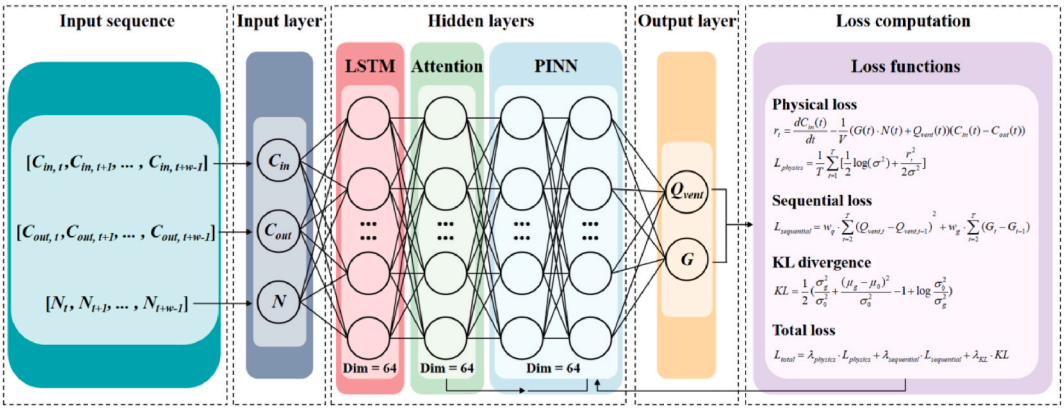

Fig. 2. Schematic diagram of proposed NVR-PINN.

PINN significantly reduces data dependency and can infer hidden variables that are not directly measured. Compared to a single PINN or LSTM structure, this hybrid structure combines their respective strengths. This enables more effective learning of the temporal dynamics of natural ventilation rates and reduces dependence on large amounts of training data. Fig. 2 shows a schematic diagram of the proposed NVR-PINN structure.

To be more specific, temporal observations of indoor CO_2 concentration C_{in}, outdoor CO_2 concentration C_{out}, and the number of occupants N are stacked over a defined sequence window of length w and passed as input features to an LSTM layer with 64 dimensions (nodes). LSTM is combined with an attention mechanism. This ensures that the model identifies the most informative time steps characterizing the ventilation rate dynamics while capturing complex temporal dependencies. Then, the input features encoded by the LSTM and the context information processed by the attention layer are passed to the PINN. The PINN consists of a shared transformation layer that converts the attention-weighted sequence representation into physics-encoded latent features, linked to a task-specific layer that simultaneously estimates the ventilation rate Q_{vent} and CO_2 generation G. This design is similar to the EKK for a holistic comparison, and can be adjusted depending on the needs in practical applications.

By optimizing PINN through the defined loss function, the model achieves stable and physically plausible estimations of ventilation rates Q_{vent} and CO_2 generation rate G. The defined loss functions consist of 3 parts: physical loss, sequential loss, and KL divergence.

The physical residual is based on the mass balance equation:

$$r_t = \frac{dC_{in}(t)}{dt} - \frac{1}{V}(G(t)\cdot N(t) + Q_{vent}(t))(C_{in}(t) - C_{out}(t)) \tag{23}$$

The CO_2 measurement noise, which is the discrepancy between the observed and actual indoor CO_2 concentration, is considered a white noise following a Gaussian distribution $\tilde{N}(0, \sigma^2)$. Hence, the log-likelihood of all residuals in a measurement period T can be calculated by:

$$L_{physics} = \frac{1}{T}\sum_{t=1}^{T}\left[\frac{1}{2}\log(\sigma^2) + \frac{r_t^2}{2\sigma^2}\right] \tag{24}$$

The sequential loss acts as a constraint that ensures temporal consistency in the estimated ventilation rate Q_{vent} and generation rate G. It functions like a temporal smoother but also regularizes the model against overfitting to noise:

$$L_{sequential} = w_q \cdot \sum_{t=2}^{T}\left(Q_{vent,t} - Q_{vent,t-1}\right)^2 + w_g \cdot \sum_{t=2}^{T}(G_t - G_{t-1}) \tag{25}$$

Where w_q and w_g are definable coefficients.

The KL divergence regularizes the learned parameter distributions to stay close to prior beliefs. The ventilation rate is dynamic, so its prior is unknown. However, the CO_2 generation rate is usually known, though with certain uncertainty. Therefore, the real CO_2 generation rate is assumed to follow a Gaussian distribution $\tilde{N}(\mu_g, \sigma_g^2)$ with μ_g representing the mean value and σ_g characterizing the uncertainty. Its prior can be obtained from existing knowledge (e.g., reference values reported in related research), which also follows a Gaussian distribution $\tilde{N}(\mu_0, \sigma_0^2)$. The KL divergence regularizes these two distributions:

$$KL = \frac{1}{2}\left(\frac{\sigma_g^2}{\sigma_0^2} + \frac{\left(\mu_g - \mu_0\right)^2}{\sigma_0^2} - 1 + \log\frac{\sigma_0^2}{\sigma_g^2}\right) \tag{26}$$

Finally, the total loss can be calculated by:

$$L_{total} = \lambda_{physics}\cdot L_{physics} + \lambda_{sequential}\cdot L_{sequential} + \lambda_{KL}\cdot KL \tag{27}$$

Where λ is a definable coefficient.

Hence, Table 1 summarizes the architecture of this LSTM-PINN structure.

3. Case study

To validate the performance of the proposed NVR-PINN, a field experimental campaign was conducted in 2 naturally ventilated classrooms at the Universitat Politècnica de Catalunya (UPC) during November to December 2024. Fig. 3 shows photos of these

Table 1
The architecture of the proposed NVR-PINN.

Layer	Number of layer	Nodes (Input → Output)	Activation Function
Input - C_{in}, C_{out}, G	1	3	/
LSTM	1	3 → 64	Tanh, Sigmoid (internal)
Attention	1	64 → 1	Softmax
PINN	1	64 → 64	Tanh
Output - Q_{vent}, G	1	64 → 2	Softplus, Sigmod (Q_{vent} remains positive, G remains within the defined range)

classrooms and their architectural characteristics. In this field experimental campaign, a total of 6 on-site measurements were performed during the class held in these 2 rooms, with 3 measurements in each room, and each class lasted around 3 h. The occupants were primarily college students with an average age of 22. As the experiments were performed in the classes of the engineering school, the gender ratio of the students was disproportionate (80 % male students and 20 % female students). However, this does not affect the use of this case for analysis.

During the field experiment, the indoor and outdoor CO_2 concentrations were measured by a Comet U3430 sensor, respectively. Following the specifications of ASTM D6245-18 [37], one sensor was placed in the center of the classroom at 1.1 m height and 2 m away from disturbances, to measure the indoor CO_2 concentration. The other sensor was placed on the exterior windowsill to measure the CO_2 concentration of the outdoor airflow. Fig. 4 illustrates the placement and technical specifications of the measurement sensors. The sensors were turned on 15 min before each measurement to stabilize the readings. Both the indoor and outdoor CO_2 concentrations were recorded at 1-min intervals. The researcher stayed in the classroom all the time to record the changes in the number of occupants and the opening/closing of windows, also at 1-min intervals. The door remained closed during the measurements and was only opened when people entered or left the room.

Hence, the field experimental campaign obtained a total of 6 measurement datasets, each containing 200-min time series of indoor and outdoor CO_2 observations, the number of female and male occupants, and the window opening areas (Table 2). Based on these datasets, the ventilation rates for each measurement were calculated using the transient mass balance model, moving average filter (MAF), extended Kalman filter (EKF), and proposed NVR-PINN.

The estimation of the ventilation rate also requires the CO_2 generation rate of the occupants. According to Persily and Jonge [34], the individual CO_2 generation rate for female students in a sedentary state (1.2 met) is 0.228 L/min/person, and for male students is 0.288 L/min/person. The teacher's CO_2 generation rate is very close to that of students (0.276 L/min/person and 0.216 L/min/-person). Therefore, the students' CO_2 generation rates were used for the calculation.

For MAF and NVR-PINN, a 10-min sequence window length (w) was used in the estimation. For EKF and NVR-PINN, the uncertainties in the CO_2 generation rate can be taken into account. According to Persily and Jonge [34], the CO_2 generation rate varies by about 15 % between activity levels. Besides, a small individual difference of 10 % was also considered and modeled. Consequently, the total uncertainty can be considered as ± 25 % of the reference value. Moreover, EKF and NVR-PINN can model CO_2 measurement noises. The CO_2 sensor used in this study has a measurement error of ±50 ppm, which is similar to other common commercial CO_2 sensors. The measurement error of the sensor is typically considered to follow the "2 sigma" principle. Therefore, the CO_2 measurement noise was considered a white noise with a sigma (σ) of 25.

In addition, since the volumes of the classrooms are different, the calculated ventilation rate Q_{vent} (m^3/min) was converted to air changes per hour (ACH) for visualization and comparison based on the equation below:

$$ACH = \frac{60 \cdot Qvent}{V} \tag{28}$$

The calculation and analysis were performed on the Google Colab platform using Python 3.10. The Numpy, Pandas, SciPy, and PyTorch libraries were used for data processing, model development, and calculation, while the Matplotlib package was used for results visualization.

4. Results and discussion

This section first presents the field measurement observations (Section 4.1). Subsequently, the ventilation rates (Section 4.2) and CO_2 concentrations (Section 4.3) estimated by the previously introduced techniques are compared, while the estimated CO_2 generation rates are also analyzed (Section 4.4). Finally, the implications and limitations of the obtained results are further discussed (Section

Architectural characteristics

Room	Floor	Floor area (m²)	Height (m)	Facade orientation	Number of window	Window area (m²)	Number of door	Door area (m²)
A	1	55.6	3.8	N	2	1.09	1	2.12
B	2	78.0	3.2	N	4	0.85	1	1.89

Fig. 3. Classroom photos and architectural characteristics.

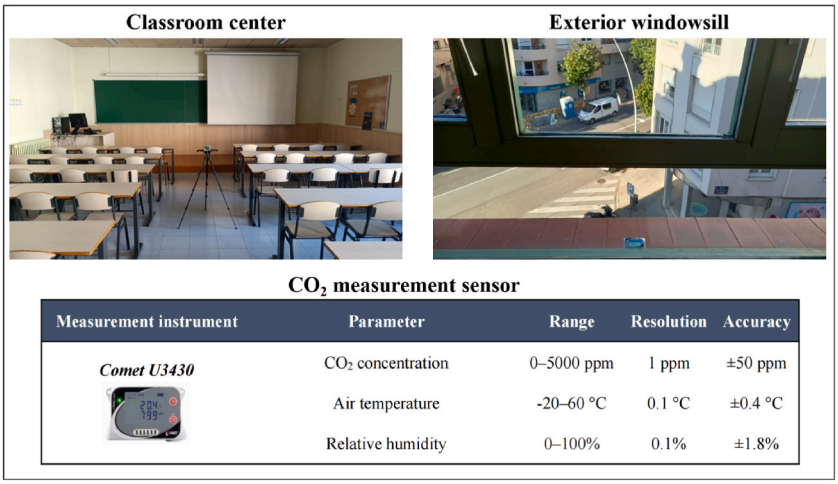

Fig. 4. CO_2 measurement sensor placement and technical specifications.

Table 2
Observations contained in each measurement dataset.

Observations	Abbreviation	Unit	Length
Indoor CO_2 concentration	C_{in}	ppm	200-min
Outdoor CO_2 concentration	C_{out}	ppm	200-min
Number of female occupants	N_f	/	200-min
Number of male occupants	N_m	/	200-min
Window opening area	WOA	m^2	200-min

4.5).

4.1. Field measurement observations

Fig. 5 presents the time series observations of indoor and outdoor CO_2 concentrations, the number of occupants, and the window opening area of the 6 measurements, each with 200 time steps. The measured indoor CO_2 concentrations ranged from 471 to 1641 ppm, while the pattern depends on occupancy and window operation. Outdoor CO_2 concentrations fluctuate between 385 and 459 ppm, with an average concentration of 420 ppm. This value is consistent with the atmospheric CO_2 concentration reported by NOAA [35]. In general, the number of occupants in classroom A was higher than that in classroom B. The occupancy of the classrooms is affected by the teaching schedule, some with short breaks in the middle of the class (e.g., A-1, A-2, and B-1), while sometimes a few students leave the class earlier (e.g., B-1 and A-3). The openable window area of classroom B is nearly 1 time larger than that of classroom A, while the window operation in each measurement was different.

4.2. Ventilation rate estimations

Based on the collected observations, the ventilation rate was estimated using the transient mass balance model, moving average filter (MAF), extended Kalman filter (EKF), and the proposed NVR-PINN, as shown in Fig. 6. Notably, in order to better observe the impact of window operation and occupancy changes on the estimated results, the window opening period and the time of occupancy change are highlighted using green and orange background colors, respectively. In addition, high-resolution zoom-in plots are presented to illustrate the key features of the ventilation rates estimated by each technique.

As can be seen, the ventilation rate calculated directly by the transient mass balance model is very unstable due to CO_2 measurement noise, with large oscillations. This certainly affects the quality of the estimated ventilation rate data in practical applications. As a simple and effective tool, MAF filtered out substantial amounts of the measurement noise, thus the fluctuations in the estimated ventilation rate were significantly reduced. However, it can be observed that MAF cannot effectively track sudden changes in the ventilation rates, while there was always a 5-min delay in the estimated ventilation rate when it suddenly increased due to the opening of windows. This is because MAF uses a 10-min sequence window to smooth CO_2 observations, which averages the neighboring values of 5 min before and after. As a recursive Bayesian filter, EKF effectively addressed CO_2 measurement noise and tracked changes in ventilation rate with the "one-step-ahead" prediction and update strategy. However, since the EKF is based entirely on CO_2 observations from 1 min before and after, it is sensitive to abrupt changes in CO_2 concentrations. This results in larger fluctuations in the estimated ventilation rate than with the MAF. Total variation is a proper metric for quantifying the overall oscillation (variability) of

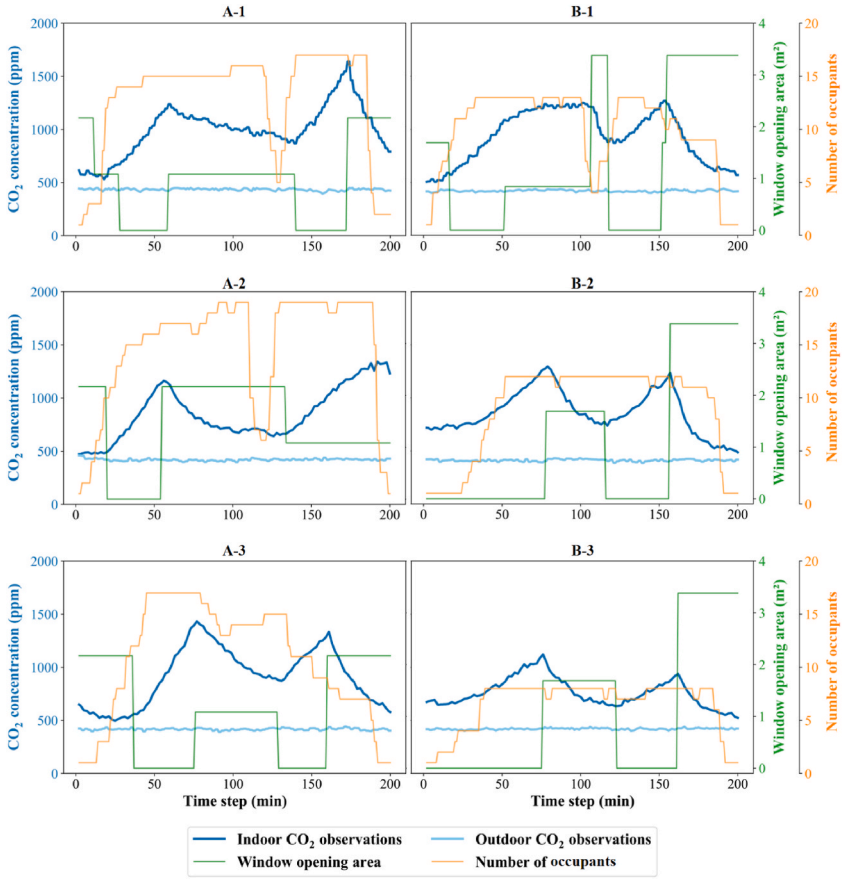

Fig. 5. Overview of measurement observations.

the curve. On average, the total variation of the ventilation rate calculated by the transient mass balance model reaches 1315. The value is 503 for EKF and only 186 for MAF.

In contrast, NVR-PINN combines the advantages of both MAF and EKF. It processes the entire time series with a 10-min sequence window, estimating the ventilation rate while handling the CO_2 measurement noises instead of simply "averaging" CO_2 observations, which better copes with the dynamics of CO_2 and natural ventilation rates. The ventilation rates estimated by NVR-PINN followed the same pattern as EKF, but were more stable and consistent. NVR-PINN achieved the lowest total variation among all techniques, with only 137. These results suggest that NVR-PINN is capable of effectively detecting sudden changes in the ventilation rate while providing stable, smooth estimates. It is also worth mentioning that during the period when the windows were closed, both MAF and EKF produced very unstable estimations and often had an estimate of 0. This is unrealistic enough because there is always a small infiltration in the space, even when the windows and doors are all closed. In contrast, the NVR-PINN estimated a very small and stable ventilation rate, which is more in line with reality.

It should also be noted that MAF cannot smooth the initial and last 5 min of CO_2 observations to estimate the ventilation rate because it smooths CO_2 concentrations with neighboring observations of 5 min before and after. Since NVR-PINN processes the entire time series with a 10-min sequence window, the first 10 min of observations are used for initialization, thereby valid estimates start 10 min later. For visualization purposes, these missing values were simply filled with the neighboring values. In practical applications, the collection of measurement data should take into account the additional observations required by these ventilation rate estimation techniques.

4.3. CO_2 concentration estimations

Fig. 7 shows the original observations of indoor CO_2 concentration and the actual CO_2 concentrations estimated by the moving average filter (MAF), extended Kalman filter (EKF), and NVR-PINN. Similarly, the window opening period and the time of occupancy change are highlighted using green and orange background colors, respectively.

The MAF averages the CO_2 observations over a 10-min sequence window. On average, the smoothed CO_2 concentration is only 1 ppm lower than the original CO_2 observations, thus perfectly following the original observations. This indicates that this technique did not adequately address the CO_2 measurement uncertainties. EKF can incorporate the measurement error of the CO_2 sensor to handle

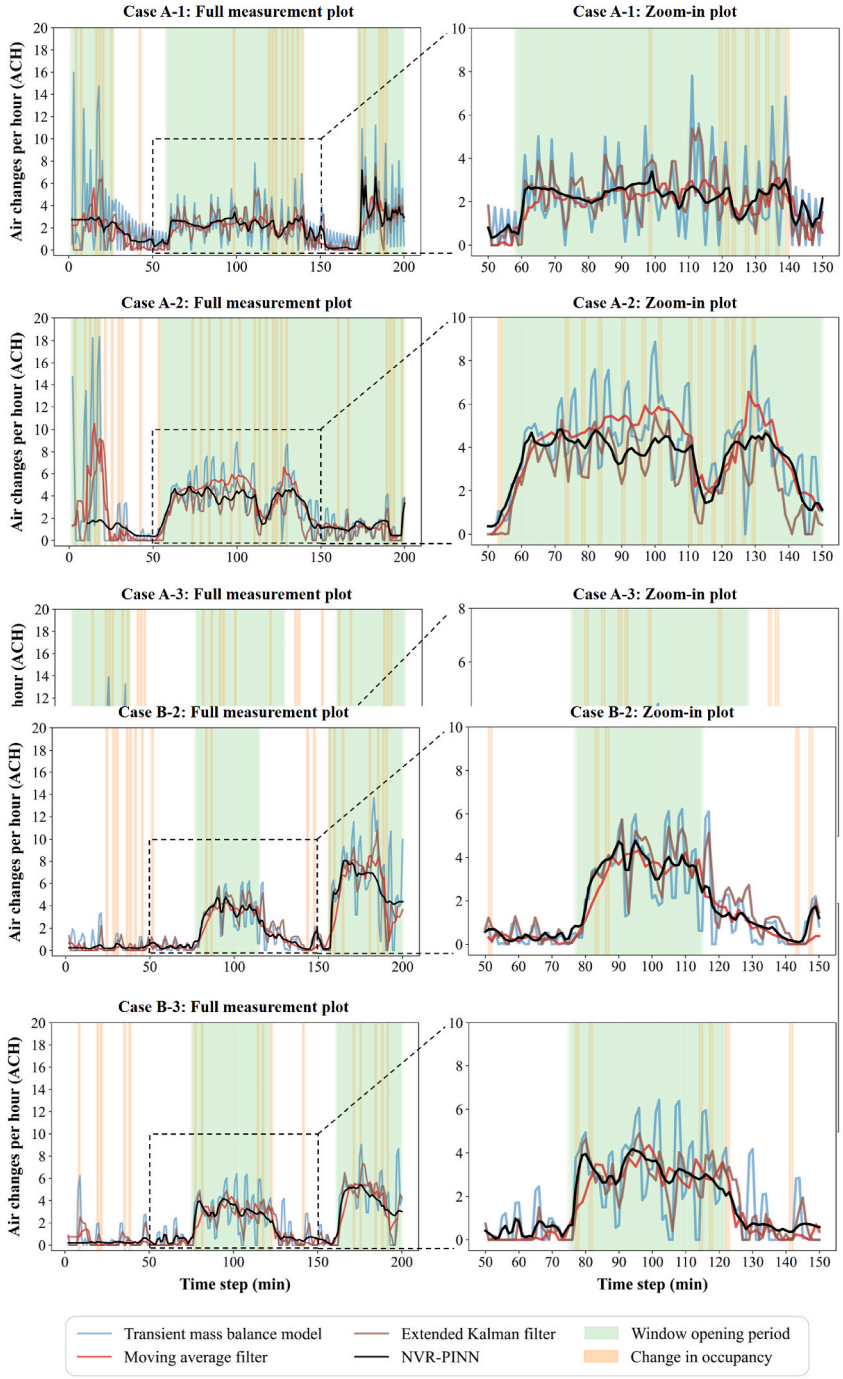

Fig. 6. Comparison of estimated ventilation rates.

measurement uncertainties. However, EKF is very sensitive to abrupt changes in CO_2 observations, as it is based on "one-step-ahead" recursive estimation. It often estimates very high ventilation rates, thereby the estimated actual CO_2 concentration was found to be significantly lower than the original CO_2 observations in many cases (e.g., B1, A2, A3, and B3). On average, the estimated CO_2 concentration was 30.3 ppm lower than the observed values. In contrast, NVR-PINN combines the advantages of both methods. It takes into account the CO_2 measurement errors, but processes the entire time series over a 10-min sequence window. It estimated more stable and consistent ventilation rates, so the calculated actual CO_2 concentration was always between MAF and EKF, better fitting the original CO_2 observation pattern. The estimated actual CO_2 concentration was 13.4 ppm lower than the observed values on average.

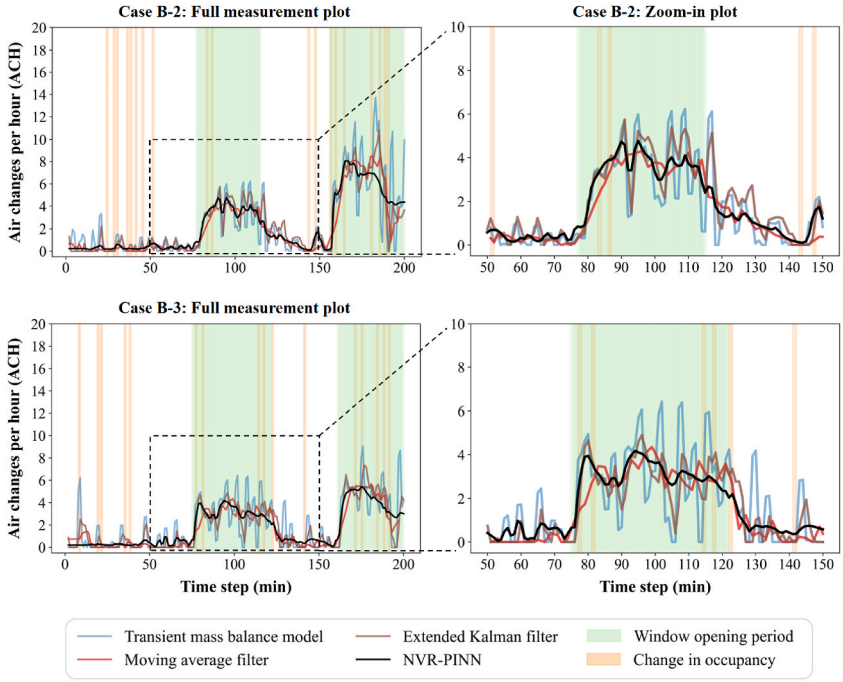

Fig. 6. (*continued*).

These results suggest that NVR-PINN is also more reliable in CO_2 measurement noise processing.

4.4. CO_2 generation rate estimations

As mentioned earlier, the transient mass balance model and the moving average filter (MAF) assume a constant CO_2 generation rate when calculating the ventilation rate. NVR-PINN is designed to function similarly to the extended Kalman filter (EKF), which can simultaneously estimate the ventilation and CO_2 generation rates while accounting for the uncertainty of the CO_2 generation rate. As introduced in the case study, the reference value of CO_2 generation rate for male students is 0.288 L/min/person, and for female students is 0.228 L/min/person. For both cases, a $\pm$25 % deviation was considered to characterize uncertainty due to individual differences and activity levels. Fig. 8 presents the CO_2 generation rates of male and female students estimated by EKF and NVR-PINN, along with the reference values and $\pm$25 % boundaries.

As can be seen, the mean values of the CO_2 generation rates estimated by EKF were consistent with the reference value for both male and female students. However, the estimation range was very large, far exceeding the upper and lower boundaries. This also suggests that EKF is unstable when applied to complex dynamic systems like natural ventilation. In contrast, the mean values of the CO_2 generation rates estimated by NVR-PINN were slightly higher than the reference values, but their ranges were narrower and completely within the upper and lower boundaries. Notably, the reference value of the CO_2 generation rate used in the case study assumes a sedentary state of occupants (1.2 met). In reality, students do not always sit still but also engage in activities such as writing or talking. In this context, their actual CO_2 generation rate should be slightly higher than the reference values. Therefore, the CO_2 generation rates estimated by NVR-PINN are also considered more consistent with the actual situation.

4.5. Further discussion on implications and limitations

It is necessary to further discuss the practical implications of the results. The original transient mass balance model does not address the noise in the CO_2 observations. The calculated ventilation rates have very large fluctuations, with poor quality for the ventilation effect analysis in practice. Although the moving average filter (MAF) is a very simple technique, it effectively reduces the amount of noise passed to the estimation of ventilation rates, demonstrating recognized practical values. However, the main limitation is that the MAF simply averages the CO_2 observations without accounting for uncertainties in CO_2 generation and measurement. Consequently, the estimated ventilation rate and CO_2 concentration may not accurately reflect the actual conditions, and there may be a delay in estimates when the ventilation rate suddenly increases. The extended Kalman filter (EKF) properly handles the CO_2 measurement noise and the CO_2 generation rate uncertainty when estimating ventilation rates. However, it is very sensitive to abrupt changes in the CO_2 observation due to the "one-step-ahead" recursive estimation, which is unstable for natural ventilation dynamics.

In contrast, the proposed NVR-PINN combines the advantages of both techniques, demonstrating better practical values. It is capable of handling both CO_2 measurement noise and CO_2 generation uncertainties, functioning with a defined sequence time window

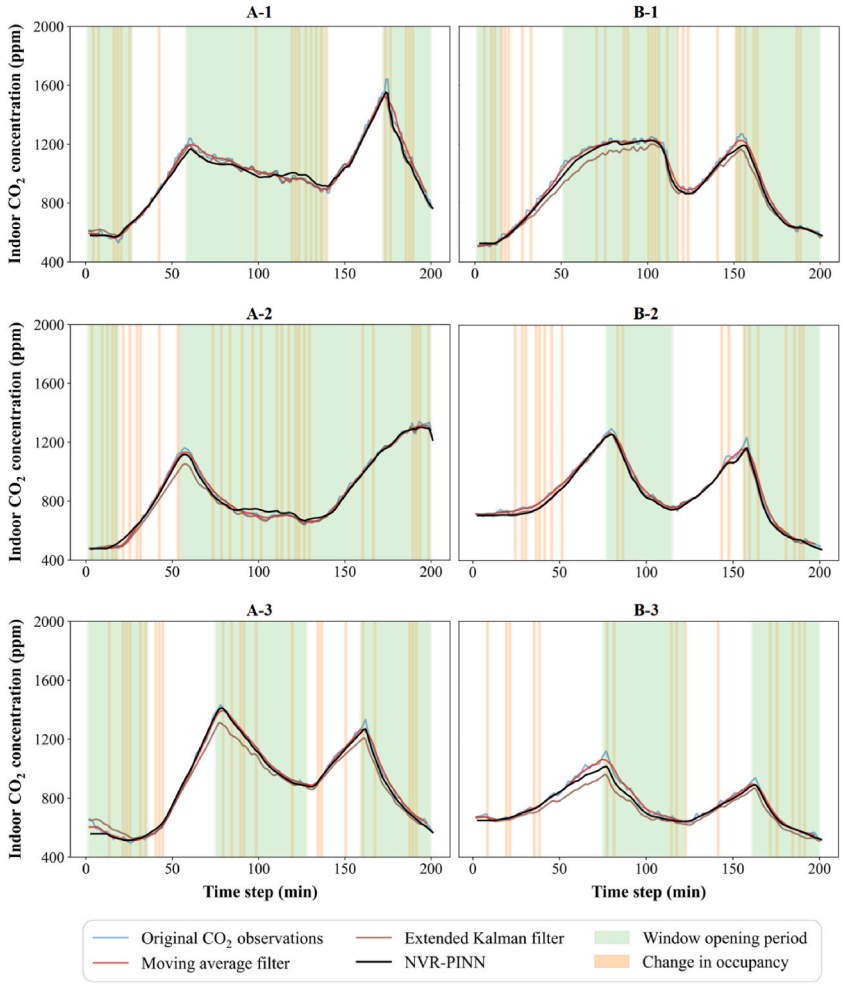

Fig. 7. Comparison of original and estimated CO_2 concentrations.

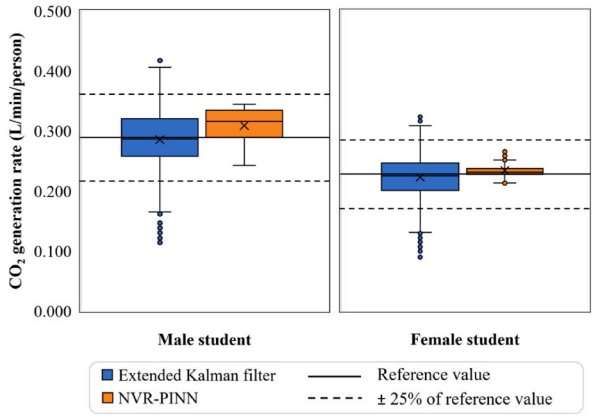

Fig. 8. Estimated CO_2 generation rate.

over the entire time series to provide more stable and consistent estimates. As a result, NVR-PINN copes better with the natural ventilation dynamics, and its estimations are more consistent with reality. Nevertheless, the NVR-PINN also has certain limitations. On the one hand, it requires an extra 10 min of observations for initialization. On the other hand, it has a more complicated model structure and requires more time for computation. In the case study, the MAF and EKF were found to be able to compute a 200-min

time series within 10 s. In contrast, the NVR-PINN requires at least 1000 epochs of iterations to reach a stabilized loss, which often takes more than 60 s.

To help with the practical application of NVR-PINN, it is also necessary to discuss the impact of sequence window length on the estimation by the proposed NVR-PINN. In the case study, the window length was defined as 10-min. Using the A-1 measurement as an example, the ventilation rates were recalculated with 5- and 15-min window lengths for comparison, as shown in Fig. 9. As can be seen, the estimated ventilation rate values were very close to each other, but the sequence window length affected the smoothness of the estimates. With a shorter window length, the model had less input information and tended to focus on "local" changes, thus the estimate comparatively fluctuates more. With a longer window length, the model focused more "globally", thereby the estimate was relatively smoother. This is actually similar to the principle of MAF. In practical applications, the definition of the window length depends on the purpose of the analysis and details of the ventilation dynamics to be retained.

Moreover, it is important to discuss the effects of CO_2 generation rates in ventilation rate estimation. When using transient mass balance model-based estimation techniques (including MAF, EKF, and the proposed NVR-PINN), it is crucial to obtain accurate CO_2 generation data with high temporal resolution, in order to ensure the accuracy of the estimated ventilation rates. Previous studies conducted in residential buildings [23,24] have demonstrated this importance. However, this can be quite challenging in educational buildings due to the presence of a large number of occupants in the classroom with changing occupancy, which ultimately leads to greater uncertainty. Accordingly, simultaneously estimating both ventilation rates and CO_2 generation rates is never recommended, even if the estimated results appear consistent with reality. In this context, Finneran and Burridge [36] proposed a new ventilation rate estimation framework that can estimate per-person ventilation rates and quantify sources of uncertainty with limited on-site occupancy information, without relying on assumptions of steady-state and uniform mixing of CO_2. This approach shows better flexibility for educational buildings. Since this research focuses on the physics-informed data-driven approach in the traditional transient mass balance model-based ventilation rate estimation, future research is recommended to further explore applications based on this new framework proposed by Finneran and Burridge [36].

Lastly, the limitations of this research should be discussed to help future research. The case study of this research was based on a field experiment conducted in real classroom environments. In this scenario, it is often difficult to directly measure the actual ventilation rates (e.g., using balometers) because this would disrupt the teaching activities. Future research is recommended to conduct experiments in controlled laboratory environments to measure actual ventilation rates. This would not only allow actual ventilation rates to be incorporated into the PINN structure as benchmark information, but also provide a more accurate CO_2 generation rates estimates as the reference for relevant research.

5. Conclusions and recommendations

This paper proposes an LSTM-PINN model for CO_2-based natural ventilation rate estimation. The performance of the proposed model was validated through a case study and compared with the existing commonly used techniques.

The results show that, since the original transient mass balance model does not address measurement noise in CO_2 observations, the calculated ventilation rates fluctuate greatly, with poor quality for ventilation effect analysis. As a simple technique, the moving average filter (MAF) can substantially alleviate the impact of CO_2 measurement noise on ventilation rate estimation, demonstrating certain practical values. However, this technique simply averages the CO_2 observations without considering the uncertainty in CO_2 generation and measurement. The estimated ventilation rate cannot accurately reflect the actual situation, and the estimates may be delayed due to the averaging of CO_2 observations. The extended Kalman filter (EKF) can properly handle CO_2 measurement noise and CO_2 generation rate uncertainty. However, this technique is not stable enough for natural ventilation dynamics due to its sensitivity to abrupt changes in CO_2 observations. In contrast, the proposed NVR-PINN combines the advantages of both techniques. It is capable of handling CO_2 measurement noise and CO_2 generation uncertainty, while processing the entire time series with a defined sequence window to provide more stable and consistent estimates of ventilation rate. As a result, the NVR-PINN can better cope with natural ventilation dynamics, with better practical values. Compared with the existing transient mass balance model and EKF, the estimation stability shown by the total variation improved by nearly 10 and 4 times, respectively, while capturing sudden changes in ventilation dynamics that MAF cannot properly reflect.

The study mainly examined the application of the proposed model from the perspective of post-processing (i.e., the ventilation rate estimation based on the field measurement data) based on field experiment in the classrooms. Future research is recommended to further explore the combination of the proposed model with the Internet of Things (IoT) monitoring sensors for the real-time natural ventilation rate estimation, and conduct the experiement in controlled laboratory environments to benchmark ventilation rates and CO_2 generation rates.

CRediT authorship contribution statement

Sen Miao: Writing – review & editing, Writing – original draft, Visualization, Validation, Methodology, Investigation, Formal analysis, Data curation, Conceptualization. **Marta Gangolells:** Writing – review & editing, Supervision, Project administration, Funding acquisition, Conceptualization. **Blanca Tejedor:** Writing – review & editing, Supervision, Conceptualization.

Declaration of competing interest

The authors declare that they have no known competing financial interests or personal relationships that could have appeared to

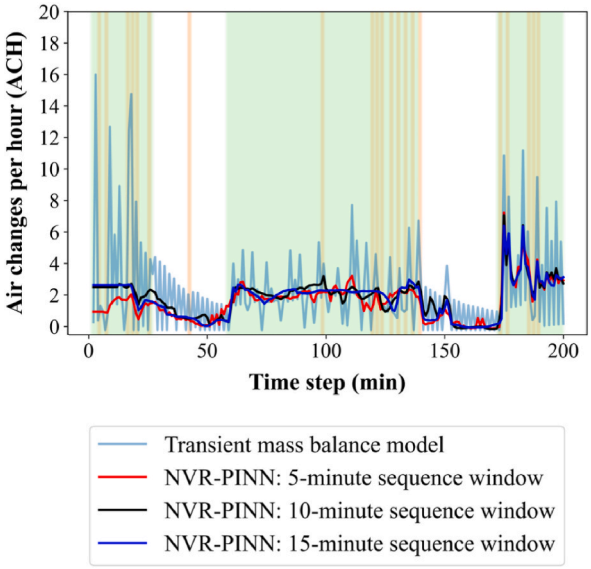

Fig. 9. Estimated ventilation rates by NVR-PINN with different sequence windows.

influence the work reported in this paper.

Acknowledgments

This research is part of the R&D project IAQ4EDU, reference no. PID2020-117366RB-I00, funded by MCIN/AEI/10.13039/501100011033. This work was supported by the Catalan Agency AGAUR under their research group support program (2021 SGR 00341). The author Sen Miao is funded by the China Scholarship Council (CSC) as a full-time PhD student, reference no. 202208390065.

Data availability

Data will be made available on request.

References

[1] CEN, EN 16798-1:2019, Part 1: indoor environmental input parameters for design and assessment of energy performance of buildings addressing indoor air quality. Thermal Environment, Lighting and Acoustics, European Committee for Standardization (CEN), Brussels, 2019.
[2] ASHRAE, ASHRAE 62.1: Ventilation and Acceptable Indoor Air Quality, The American Society of Heating, Refrigerating and Air-Conditioning Engineers (ASHRAE), Atlanta, 2022.
[3] T.S. Larsen, C. Plesner, V. Leprince, F.R. Carrié, A.K. Bejder, Calculation methods for single-sided natural ventilation: now and ahead, Energy Build. 177 (2018) 279–289, https://doi.org/10.1016/j.enbuild.2018.06.047.
[4] H.Y. Zhong, Y. Sun, J. Shang, F.P. Qian, F.Y. Zhao, H. Kikumoto, C. Jimenez-Bescos, X. Liu, Single-sided natural ventilation in buildings: a critical literature review, Build. Environ. 212 (2022) 108797, https://doi.org/10.1016/j.buildenv.2022.108797.
[5] S. Batterman, Review and extension of CO_2-based methods to determine ventilation rates with application to school classrooms, Int. J. Environ. Res. Public Health. 14 (2) (2017) 145, https://doi.org/10.3390/ijerph14020145.
[6] G. Remion, B. Moujalled, M. El Mankibi, Review of tracer gas-based methods for the characterization of natural ventilation performance: comparative analysis of their accuracy, Build. Environ. 160 (2019) 106180, https://doi.org/10.1016/j.buildenv.2019.106180.
[7] W.W. Nazaroff, Residential air-change rates: a critical review, Indoor Air 31 (2) (2021) 282–313, https://doi.org/10.1111/ina.12785.
[8] M. de Jode, Long term monitoring of CO_2 levels and ventilation rates in a naturally ventilated residential apartment, Indoor Environments 1 (3) (2024) 100030, https://doi.org/10.1016/j.indenv.2024.100030.
[9] M. Macarulla, M. Casals, N. Forcada, M. Gangolells, A. Giretti, Estimation of a room ventilation air change rate using a stochastic grey-box modelling approach, Measurement 124 (2018) 539–548, https://doi.org/10.1016/j.measurement.2018.04.029.
[10] A. Asif, M. Zeeshan, Comparative analysis of indoor air quality in offices with different ventilation mechanisms and simulation of ventilation process utilizing system dynamics tool, J. Build. Eng. 72 (2023) 106687, https://doi.org/10.1016/j.jobe.2023.106687.
[11] D.L. Johnson, R.A. Lynch, E.L. Floyd, J. Wang, J.N. Bartels, Indoor air quality in classrooms: environmental measures and effective ventilation rate modeling in urban elementary schools, Build. Environ. 136 (2018) 185–197, https://doi.org/10.1016/j.buildenv.2018.03.040.
[12] A. Asif, M. Zeeshan, Indoor temperature, relative humidity and CO2 monitoring and air exchange rates simulation utilizing system dynamics tools for naturally ventilated classrooms, Build. Environ. 180 (2020) 106980, https://doi.org/10.1016/j.buildenv.2020.106980.
[13] S.S. Korsavi, A. Montazami, D. Mumovic, Ventilation rates in naturally ventilated primary schools in the UK; contextual, occupant and Building-related (COB) factors, Build. Environ. 181 (2020) 107061, https://doi.org/10.1016/j.buildenv.2020.107061.
[14] M. Gil-Baez, J. Lizana, J.A. Becerra Villanueva, M. Molina-Huelva, A. Serrano-Jimenez, R. Chacartegui, Natural ventilation in classrooms for healthy schools in the COVID era in mediterranean climate, Build. Environ. 206 (2021) 108345, https://doi.org/10.1016/j.buildenv.2021.108345.
[15] M. Shrestha, H.B. Rijal, G. Kayo, M. Shukuya, An investigation on CO_2 concentration based on field survey and simulation in naturally ventilated Nepalese school buildings during summer, Build. Environ. 207 (2022) 108405, https://doi.org/10.1016/j.buildenv.2021.108405.

[16] R. Duarte, M. Glória Gomes, A. Moret Rodrigues, Estimating ventilation rates in a window-aired room using Kalman filtering and considering uncertain measurements of occupancy and CO_2 concentration, Build. Environ. 143 (2018) 691–700, https://doi.org/10.1016/j.buildenv.2018.07.016.
[17] A. Kabirikopaei, J. Lau, Uncertainty analysis of various CO_2-Based tracer-gas methods for estimating seasonal ventilation rates in classrooms with different mechanical systems, Build. Environ. 179 (2020) 107003, https://doi.org/10.1016/j.buildenv.2020.107003.
[18] J. Kang, K.I. Hwang, A comprehensive real-time indoor air quality level indicator, Sustainability 8 (9) (2016) 881, https://doi.org/10.3390/su8090881.
[19] A. Mohammadshirazi, V.A. Kalkhorani, J. Humes, B. Speno, J. Rike, R. Ramnath, J.D. Clark, Predicting airborne pollutant concentrations and events in a commercial building using low-cost pollutant sensors and machine learning: a case study, Build. Environ. 213 (2022) 108833, https://doi.org/10.1016/j.buildenv.2022.108833.
[20] S. Miao, M. Gangolells, B. Tejedor, Assessing the fluctuation of indoor thermal conditions in naturally ventilated classrooms through k-means clustering, Indoor Air 2025 (2025) 4453536, https://doi.org/10.1155/ina/4453536.
[21] S. Miao, M. Gangolells, B. Tejedor, Investigating students' subjective comfort with window-airing during the cold season: thermal sensation, humidity, air movement, and perceived air quality, Build. Environ. 278 (2025) 112988, https://doi.org/10.1016/j.buildenv.2025.112988.
[22] G. Remion, B. Moujalled, M. El Mankibi, Dynamic measurement of the airflow rate in a two-zones dwelling, from the CO_2 tracer gas-decay method using the Kalman filter, Build. Environ. 188 (2021) 107493, https://doi.org/10.1016/j.buildenv.2020.107493.
[23] S. Liu, Y. Jian, J. Liu, R. Guo, W. Zhu, Associating occupants' interaction with windows with air change rate –One case study, Build. Environ. 222 (2022) 109387, https://doi.org/10.1016/j.buildenv.2022.109387.
[24] Y. Jian, X. Shao, X. Gai, S. Liu, C. Chen, S. Liu, Multizone representation of time-varying airflows in naturally ventilated dwellings: occupant-generated CO_2 approach, Energy Build. 308 (2024) 114038, https://doi.org/10.1016/j.enbuild.2024.114038.
[25] Y. Zhu, S.A. Al-Ahmed, M.Z. Shakir, J.I. Olszewska, LSTM-based IoT-enabled CO_2 steady-state forecasting for indoor air quality monitoring, Electronics 12 (1) (2022) 107, https://doi.org/10.3390/electronics12010107.
[26] G. Yang, E. Yuan, W. Wu, Predicting the long-term CO_2 concentration in classrooms based on the BO–EMD–LSTM model, Build. Environ. 224 (2022) 109568, https://doi.org/10.1016/j.buildenv.2022.109568.
[27] H. Yao, X. Shen, W. Wu, Y. Lv, V. Vishnupriya, H. Zhang, Z. Long, Assessing and predicting indoor environmental quality in 13 naturally ventilated urban residential dwellings, Build. Environ. 253 (2024) 111347, https://doi.org/10.1016/j.buildenv.2024.111347.
[28] G.E. Karniadakis, I.G. Kevrekidis, L. Lu, et al., Physics-informed machine learning, Nat. Rev. Phys. 3 (2021) 422–440, https://doi.org/10.1038/s42254-021-00314-5.
[29] F. Arnold, R. King, State–space modeling for control based on physics-informed neural networks, Eng. Appl. Artif. Intell. 101 (2021) 104195, https://doi.org/10.1016/j.engappai.2021.104195.
[30] R.E. Kalman, A new approach to linear filtering and prediction problems, J. Basic Eng 82 (1) (1960) 35–45, https://doi.org/10.1115/1.3662552.
[31] J. Mochnac, S. Marchevsky, P. Kocan, Bayesian filtering techniques: Kalman and extended Kalman filter basics. 19th International Conference Radioelektronika, IEEE Explore, 2009, pp. 119–122, https://doi.org/10.1109/radioelek.2009.5158765.
[32] R.R. Labbe, Kalman and Bayesian filters in python, Available at: https://github.com/rlabbe/Kalman-and-Bayesian-Filters-in-Python, 2020.
[33] S. Hochreiter, J. Schmidhuber, Long short-term memory, Neural Comput. 9 (8) (1997) 1735–1780, https://doi.org/10.1162/neco.1997.9.8.1735.
[34] A. Persily, L. Jonge, Carbon dioxide generation rates for building occupants, Indoor Air 27 (5) (2017) 868–879, https://doi.org/10.1111/ina.12383.
[35] NOAA, Trends in atmospheric carbon dioxide (CO2), Available at: https://gml.noaa.gov/ccgg/trends/, 2024. (Accessed 10 December 2024).
[36] J. Finneran, H.C. Burridge, Inferring ventilation rates with quantified uncertainty in operational rooms using point measurements of carbon dioxide: classrooms as a case study, Build. Environ. 254 (2024) 111309, https://doi.org/10.1016/j.buildenv.2024.111309.
[37] ASTM, Astm D6245-18. Standard Guide for Using Indoor Carbon Dioxide Concentrations to Evaluate Indoor Air Quality and Ventilation, American Society for Testing and Materials (ASTM), Pennsylvania, 2018.